

Static assessment of quadratic hybrid plane stress element using non-conforming displacement modes and modified shape functions

Kyoung-Sik Chun[†]

Structural Division, BAU CONSULTANT Co., Ltd., 968-5 Daechi-dong, Gangnam-gu, Seoul 135-736, Korea

Samuel Kinde Kassegne[‡]

Department of Mechanical Engineering, San Diego State University, 5500 Campanile Dr., San Diego, CA 92182, United States

Won-Tae Park^{‡†}

Division of Construction and Environmental Engineering, Kongju National University, 275 Budae-dong, Cheonan-si, Chungnam 330-717, Korea

(Received November 21, 2007, Accepted June 9, 2008)

Abstract. In this paper, we present a quadratic element model based on non-conforming displacement modes and modified shape functions. This new and refined 8-node hybrid stress plane element consists of two additional non-conforming modes that are added to the translational degree of freedom to improve the behavior of a membrane component. Further, the modification of the shape functions through quadratic polynomials in x - y coordinates enables retaining reasonable accuracy even when the element becomes considerably distorted. To establish its accuracy and efficiency, the element is compared with existing elements and - over a wide range of mesh distortions - it is demonstrated to be exceptionally accurate in predicting displacements and stresses.

Keywords: hybrid element; assumed stress; 8-node plane stress element; modified shape function; non-conforming displacement modes.

1. Introduction

For several decades, considerable efforts have been devoted to the development of finite elements with good performance, especially, of enhanced accuracy in coarse meshes and free of spurious locking. Although there are some exceptions, most of these finite elements can generally be grouped

[†] Manager, Corresponding author, E-mail: chunks@dreamwiz.com

[‡] Assistant Professor, E-mail: kassegne@mail.sdsu.edu

^{‡†} Associate Professor, E-mail: pwtae@kongju.ac.kr

into two distinct classes of element models. These models are the displacement model, which is basically based on the total potential energy principle and the mixed model, which - in addition to displacements - assumes one or more independent fields such as stresses or strains.

Developments in mixed/hybrid plane elements have been particularly extensive and form the focus of this study. Beginning with the assumed stress hybrid finite element proposed by Pian (1964), numerous additional formulations have been developed. The major challenge in deriving hybrid finite elements seems to be the lack of a rational way for deriving the optimal stress modes. Recently, several partial hybrid finite elements have been proposed with a variety of methods for deriving assumed stress fields. Pian and Sumihara (1984) proposed a new approach for hybrid stress elements that is based on the Hellinger-Reissner principle. They defined the assumed stresses in the natural coordinate system. The stresses are in-turn initially defined in the form of complete uncoupled polynomials. Equilibrium conditions are then enforced on them through integral-type equations with geometric perturbation and subsequently degenerated to optimal stress terms. As modified versions of this scheme, Pian and Tong (1986), and Pian and Wu (1988) proposed new constraint equations for assumed stresses which did not need geometrical perturbation to obtain the sufficient number of constraint equations. Their initial choice of stress terms are unconstrained and complete polynomials. The additional displacements are used as Lagrange multipliers to enforce the stress equilibrium constraint.

Recently, Sze (1992) used orthogonal lower- and higher-order stress modes to construct a hybrid element. His approach allows the partition of the element stiffness matrix into a lower- and a higher-order stiffness matrix. When the lower-order stiffness turns out to be identical to the sub-integrated element, the higher-order stiffness matrix plays the role of a stabilization matrix. A more general hybrid model was developed by Chen and Cheung (1995) who proposed a new approach for approximation of the assumed stresses. The key to their approach lies in rational choice of the incompatible modes containing first-order terms which are introduced to relax the sensitivity to mesh distortion. Wu and Cheung (1995, 1996) presented a penalty equilibrium term for enforcing equilibrium conditions in a variational sense. Di and Ramm (1994) introduced a rigorous unified formulation of stress interpolations without non-conforming modes. They investigated a series of hybrid elements based on Hellinger-Reissner principle. Their formulations – which are unique in the way the stress assumptions are chosen – are based on the normalized stress transformation and the concept of directly interpolating the physical components of the stress tensor. Yeo and Lee (1997) proposed the generalized non-compatible displacements modes for a refined four-node hybrid stress plane element and eight-node hybrid stress brick element. Feng *et al.* (1997) presented a brief compilation of studies dealing with criteria for stability and convergence of hybrid finite elements. Choi *et al.* (1999) presented a defect-free 4-node flat shell element with non-conforming modes. Recently, Chun and Kassegne (2005) proposed a new, efficient 8-node serendipity element with explicit and assumed strains formulation, modified shape functions, and refined first-order theory for the static, buckling and free-vibration analysis of fibrous composite plates.

However, research in developing more refined and accurate plane elements, especially under loads and geometries leading to severe distortions, are still ongoing. In this particular study, an approach for choosing the stress terms for 8-node hybrid stress elements is selected and a new element model based on non-conforming displacement modes and modified shape functions is presented. The new and refined 8-node hybrid stress plane element presented here is then compared with existing elements to establish its accuracy and efficiency.

2. Modified shape functions

The 8-node Serendipity element can be modified so that it can represent any quadratic polynomials in x - y coordinates, thus retaining reasonable accuracy even when the element becomes considerably distorted (1999). Essentially, the concept adopted here is that of deriving 8-node element by eliminating the interior node (ninth node) of the 9-node one with all the Cartesian quadratic polynomials preserved (Kikuchi *et al.* 1999, MacNeal and Harder 1992, Chun and Kassegne 2005).

$$\delta = \sum_{i=1}^8 \bar{N}_i \delta_i \tag{1}$$

$$\bar{N}_i = N_i^{(9)} + N_9^{(9)} T_i \tag{2}$$

where the $N_i^{(9)}$ is the shape function of the i -th node in the 8-node Lagrange element and T_i is a coefficient of constraint. Eq. (2) can then be expressed in terms of standard 8-noded shape functions, $N_i^{(8)}$ and hierarchical form. Therefore,

$$\bar{N}_i = N_i^{(8)} + N_9^{(9)} (T_i - N_i^{(8)}(0, 0)) \tag{3}$$

The constraint coefficients, T_i , are constructed with the aid of x - y coordinate at each node. For convenience, the shape functions M_i^S for the 8-node Serendipity element are shown below.

$$M_i^S(\xi, \eta) = N_i(\xi, \eta) - 1/4 N_9(\xi, \eta) \tag{4}$$

$$M_{i+4}^S(\xi, \eta) = N_{i+4}(\xi, \eta) + 1/2 N_9(\xi, \eta) \tag{5}$$

The modified shape functions for the present 8-node Serendipity element are, therefore, expressed for $1 \leq i \leq 4$ as

$$M_i(\xi, \eta) = M_i^S(\xi, \eta) + \frac{D_i - D_k}{8(D_i + D_k)} N_9(\xi, \eta) \tag{6}$$

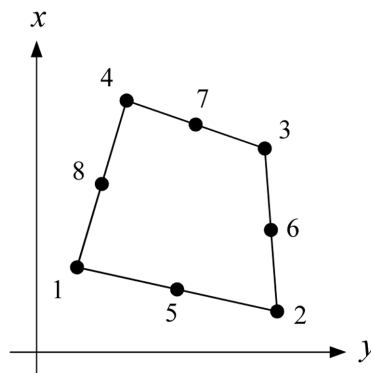


Fig. 1 An eight-node element

$$M_{i+4}(\xi, \eta) = M_{i+4}^S(\xi, \eta) + \frac{D_m - D_i}{4(D_i + D_k)} N_9(\xi, \eta) \quad (7)$$

where the natural coordinates ξ and η are equal to ± 1 on the boundaries and their values at node i , ξ_i and η_i are given by $\xi_i = -1, 1, 1, -1, 0, 1, 0, -1$ and $\eta_i = -1, -1, 1, 1, -1, 0, 1, 0$ for $i = 1, \dots, 8$, respectively. D_i is equal to four times the Jacobian $\partial(x, y)/\partial(\xi, \eta)$ at vertex i , and is defined as

$$D_i = \begin{vmatrix} x_j - x_i & x_m - x_i \\ y_j - y_i & y_m - y_i \end{vmatrix} \quad (8)$$

$$(i, j, k, m) = \text{any one of } \begin{bmatrix} (1, 2, 3, 4) & (3, 4, 1, 2) \\ (2, 3, 4, 1) & (4, 1, 2, 3) \end{bmatrix} \quad (9)$$

To enhance the original Serendipity element, Kikuchi *et al.* (1999) and MacNeal and Harder (1992) presented a modified method that includes any quadratic terms of Cartesian coordinates when the element is of convex bilinear subparametric shape.

3. Non-conforming displacement modes

A number of different techniques have been proposed for improving the basic behavior of quadrilateral elements. Among these techniques, the use of non-conforming displacement modes is among the most successful approaches in pure bending situations. The basic concept of this approach is to restore true deformation by adding additional deformation modes which are called non-conforming displacement modes (Choi *et al.* 1999).

The displacement fields of a finite element can be enhanced by adding non-conforming displacements modes to the original displacement components of the element as

$$\begin{Bmatrix} u \\ v \end{Bmatrix} = \sum_{i=1}^n M_i^S \begin{Bmatrix} u_i \\ v_i \end{Bmatrix} + \sum_{j=1}^m \bar{N}_j \begin{Bmatrix} \lambda_j \\ \lambda_{j+1} \end{Bmatrix} \quad (10)$$

where M_i^S represents the explicit modified shape functions and \bar{N}_j is the vector of non-conforming shape functions as defined in Eqs. (6), (7). The number of nodes per element is given by 'n', and m is the number of the non-conforming displacement fields. The possible non-conforming displacement modes to be added to an 8-node Serendipity element are shown in Fig. 2 and defined by the following set of shape functions (Choi and Park 1999)

$$\begin{aligned} \bar{N}_1 &= \xi(1 - \xi^2), & \bar{N}_2 &= \eta(1 - \eta^2), & \bar{N}_3 &= (1 - \xi^2)(1 - \eta^2) \\ \bar{N}_4 &= \xi\eta(1 - \xi^2), & \bar{N}_5 &= \xi\eta(1 - \eta^2) \end{aligned} \quad (11)$$

The modes in Eq. (11) are selected to have zero values at each node and eliminate the undesirable constraints present in an original isoparametric element. The first two modes in Eq. (11) are used to introduce cubic polynomials, the third mode adds the bubble shape displacement, and the fourth and fifth modes contribute to the softening of twisting constraints to the element (Choi and Park 1999).

The establishment of various improved elements is possible by selectively adding non-conforming modes \bar{N}_j . The quadratic plate-bending elements which have three non-conforming modes (\bar{N}_1, \bar{N}_2 and \bar{N}_3) and five modes ($\bar{N}_1 - \bar{N}_5$) are presented by Choi and Park (1999). In this research, two

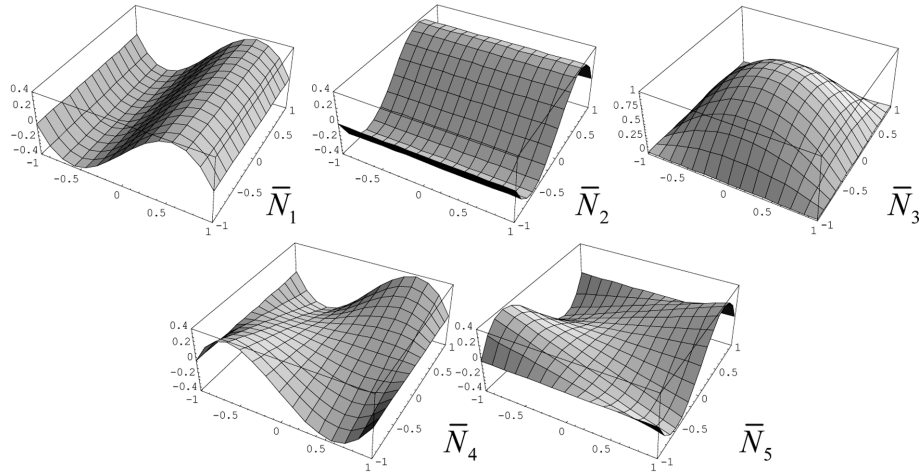


Fig. 2 Non-conforming displacement modes for quadratic element

more non-conforming modes (\bar{N}_1, \bar{N}_2) are added to the translational degree of freedom to improve the behavior of a membrane element. Therefore, the hybrid assumed stress fields proposed here are based on the combinations of the non-conforming displacement modes by Pian and Wu (1988) and Chen and Cheung (1995). It is now well-established that the formulation of hybrid stress element based on the vanishing of the virtual work due to the higher order stresses and incompatible displacements along the element boundary lead to satisfactory elements (Pian and Wu 1988). Further, when the incompatible displacements also satisfy the constant strain patch test the resulting elements will provide the most accurate solutions. Pian and Wu (1988) reviewed briefly recent developments in using the added incompatible displacements to formulate hybrid stress elements, in which relations between the hybrid stress model and the corresponding incompatible displacement model are emphasized. The assumed stresses initially are all chosen to be complete in linear terms in natural coordinates. The equilibrium conditions are imposed in a variational sense through the internal displacements which are also expanded in the natural coordinates. The resulting element possesses the rational stress terms, i.e., it is invariant, it is less sensitive to geometric distortion, and contains a minimum number of stress parameters.

4. Assumed stress formulations

Recently, many rational approaches for stress assumption have been forwarded for hybrid stress elements. The main feature of these approaches is the adoption of constraint equations for assumed stresses. Among them, Pain and Tong (1986) proposed the following constraint equations for higher-order terms of assumed stresses

$$\int_{\Omega} (D \delta \mathbf{u}_{\lambda})^T \boldsymbol{\sigma}_h d\Omega = 0 \quad (12)$$

where $\boldsymbol{\sigma}_h$ is the higher-order terms in the assumed stresses, $\delta \mathbf{u}_{\lambda}$ is the admissible variation of the non-conforming modes and D is the differential operator of the strain-displacement equations. Eq. (12) suggests that the higher-order terms should be orthogonal to the non-conforming strains

and was employed by Chen and Cheung (1995) to 4-node plane element.

For 4-node plane element, if the following non-conforming modes (Eq. (13)) of Wilson *et al.* (1973) and Taylor *et al.* (1976) are considered,

$$\mathbf{u}_\lambda = \begin{Bmatrix} (1 - \xi^2)\lambda_1 + (1 - \eta^2)\lambda_2 \\ (1 - \xi^2)\lambda_3 + (1 - \eta^2)\lambda_4 \end{Bmatrix} \tag{13}$$

and Eq. (1) employed, then the resulting stress assumption is found to be the same with that of Pian and Sumihara (1984). The stresses σ_e are expanded in terms of assumed stress parameters β .

$$\sigma_e = (\mathbf{I}_c + \hat{\mathbf{P}}_h)\boldsymbol{\beta} = \begin{bmatrix} 1 & 0 & 0 & \vdots & a_1^2\eta & a_3^2\xi \\ 0 & 1 & 0 & \vdots & b_1^2\eta & b_3^2\xi \\ 0 & 0 & 1 & \vdots & a_1b_1\eta & a_3b_3\xi \end{bmatrix} \begin{Bmatrix} \beta_1 \\ \vdots \\ \beta_5 \end{Bmatrix} \tag{14}$$

where \mathbf{I}_c is a 3×3 identity matrix. The coefficients a_i and b_i can be expressed in terms of nodal coordinates, x_i and y_i .

$$\begin{bmatrix} a_1 & b_1 \\ a_2 & b_2 \\ a_3 & b_3 \end{bmatrix} = \frac{1}{4} \begin{bmatrix} -1 & 1 & 1 & -1 \\ 1 & -1 & 1 & -1 \\ -1 & -1 & 1 & 1 \end{bmatrix} \begin{Bmatrix} x_1 & y_1 \\ \vdots & \vdots \\ x_4 & y_4 \end{Bmatrix} \tag{15}$$

For 8-node quadratic element, the initial interpolation for the stress field σ_e is obtained by inspecting the polynomial terms contained in the strain field. The assumed stresses are initially taken to be of complete second order in ξ and η , i.e.,

$$\begin{aligned} \sigma_e &= (\mathbf{I}_c + \mathbf{P}_h)\boldsymbol{\beta} \\ &= \begin{bmatrix} 1 & 0 & 0 & \vdots & \xi & 0 & 0 & \eta & 0 & 0 & \xi\eta & 0 & 0 & \xi^2 & 0 & 0 & \eta^2 & 0 & 0 \\ 0 & 1 & 0 & \vdots & 0 & \xi & 0 & 0 & \eta & 0 & 0 & \xi\eta & 0 & 0 & \xi^2 & 0 & 0 & \eta^2 & 0 \\ 0 & 0 & 1 & \vdots & 0 & 0 & \xi & 0 & 0 & \eta & 0 & 0 & \xi\eta & 0 & 0 & \xi^2 & 0 & 0 & \eta^2 \end{bmatrix} \begin{Bmatrix} \beta_1 \\ \vdots \\ \beta_{18} \end{Bmatrix} \end{aligned} \tag{16}$$

The Jacobian matrix, $[J]$ is commonly given as

$$[J] = \begin{bmatrix} J_{11} & J_{12} \\ J_{21} & J_{22} \end{bmatrix} = \begin{bmatrix} \frac{\partial x}{\partial \xi} & \frac{\partial y}{\partial \xi} \\ \frac{\partial x}{\partial \eta} & \frac{\partial y}{\partial \eta} \end{bmatrix} = \begin{bmatrix} \frac{\partial M_1^s}{\partial \xi} & \frac{\partial M_2^s}{\partial \xi} & \cdots & \frac{\partial M_8^s}{\partial \xi} \\ \frac{\partial M_1^s}{\partial \eta} & \frac{\partial M_2^s}{\partial \eta} & \cdots & \frac{\partial M_8^s}{\partial \eta} \end{bmatrix} \begin{Bmatrix} x_1 & y_1 \\ x_2 & y_2 \\ \vdots & \vdots \\ x_8 & y_8 \end{Bmatrix} \tag{17}$$

The relations between natural coordinate ξ, η and Cartesian coordinates x, y can be determined as

$$\begin{Bmatrix} \frac{\partial}{\partial x} \\ \frac{\partial}{\partial y} \end{Bmatrix} = [j]^{-1} \begin{Bmatrix} \frac{\partial}{\partial \xi} \\ \frac{\partial}{\partial \eta} \end{Bmatrix} = \frac{1}{|j|} \begin{bmatrix} j_{22} & -j_{12} \\ -j_{21} & j_{11} \end{bmatrix} \begin{Bmatrix} \frac{\partial}{\partial \xi} \\ \frac{\partial}{\partial \eta} \end{Bmatrix} \tag{18}$$

where j denotes the Jacobian matrix in Eq. (17) evaluated at the origin $(\xi, \eta) = (0, 0)$ of the element. For the choice of \mathbf{u}_λ terms, non-conforming displacement fields are considered in Eq. (19). The non-conforming functions of quadratic elements are aforementioned.

$$\mathbf{u}_\lambda = \begin{Bmatrix} u_\lambda \\ v_\lambda \end{Bmatrix} = \begin{Bmatrix} \xi(1-\xi^2)\lambda_1 + \eta(1-\eta^2)\lambda_2 \\ \xi(1-\xi^2)\lambda_3 + \eta(1-\eta^2)\lambda_4 \end{Bmatrix} \quad (19)$$

The constraint Eq. (12) for the higher-order stress terms be expressed as

$$\begin{aligned} \int_{\Omega} (D\delta\mathbf{u}_\lambda)^T \boldsymbol{\sigma}_h d\Omega &= \iint_A \begin{bmatrix} u_{\lambda,x} \\ v_{\lambda,y} \\ u_{\lambda,y} + v_{\lambda,x} \end{bmatrix}^T \begin{bmatrix} \sigma_x \\ \sigma_y \\ \tau_{xy} \end{bmatrix} |j| td\xi d\eta \\ &= \iint_A \left[\frac{\partial u_\lambda}{\partial x} \sigma_x + \frac{\partial v_\lambda}{\partial y} \sigma_y + \left(\frac{\partial u_\lambda}{\partial y} + \frac{\partial v_\lambda}{\partial x} \right) \tau_{xy} \right] |j| td\xi d\eta \\ &= \iint_A \left[\left(j_{22} \frac{\partial u_\lambda}{\partial \xi} - j_{12} \frac{\partial u_\lambda}{\partial \eta} \right) \sigma_x + \left(-j_{21} \frac{\partial v_\lambda}{\partial \xi} + j_{11} \frac{\partial v_\lambda}{\partial \eta} \right) \sigma_y \right. \\ &\quad \left. + \left(-j_{21} \frac{\partial u_\lambda}{\partial \xi} + j_{11} \frac{\partial u_\lambda}{\partial \eta} + j_{22} \frac{\partial v_\lambda}{\partial \xi} - j_{12} \frac{\partial v_\lambda}{\partial \eta} \right) \tau_{xy} \right] td\xi d\eta = 0 \end{aligned} \quad (20)$$

To satisfy the equilibrium conditions point-wise, the coefficients of λ_1 , λ_2 , λ_3 and λ_4 in the above equation must be identically zero. That is,

$$\begin{aligned} -j_{22}\beta_7 + j_{21}\beta_{17} &= 0 \\ j_{12}\beta_8 - j_{11}\beta_{18} &= 0 \\ j_{21}\beta_{12} - j_{22}\beta_{17} &= 0 \\ -j_{11}\beta_{13} + j_{12}\beta_{18} &= 0 \end{aligned} \quad (21)$$

Based on two independent parameters β_7 and β_8 into Eq. (21), four dependent parameters can be eliminated and finally, the higher-order terms in stress fields can be found,

$$\boldsymbol{\sigma}_h = \hat{\mathbf{P}}_h \boldsymbol{\beta} \quad (22)$$

where

$$\hat{\mathbf{P}}_h = \mathbf{P}_h + \hat{\mathbf{P}}_{h2} = \begin{bmatrix} \xi & 0 & 0 & \eta & 0 & 0 & \xi\eta & 0 & 0 & \vdots & j_{21}^2 \xi^2 & j_{11}^2 \eta^2 \\ 0 & \xi & 0 & 0 & \eta & 0 & 0 & \xi\eta & 0 & \vdots & j_{22}^2 \xi^2 & j_{12}^2 \eta^2 \\ 0 & 0 & \xi & 0 & 0 & \eta & 0 & 0 & \xi\eta & \vdots & j_{21}j_{22} \xi^2 & j_{11}j_{12} \eta^2 \end{bmatrix}$$

Therefore the resulting stress assumption satisfying the constraint equations can be given as

$$\boldsymbol{\sigma}_e = \boldsymbol{\sigma}_c + \boldsymbol{\sigma}_h = \mathbf{P} \cdot \boldsymbol{\beta} = (\mathbf{I}_c + \mathbf{P}_{h1} + \hat{\mathbf{P}}_{h2}) \boldsymbol{\beta}$$

$$= \begin{bmatrix} 1 & 0 & 0 & \vdots & \xi & 0 & 0 & \eta & 0 & 0 & \xi\eta & 0 & 0 & \vdots & j_{11}^2\eta^2 & j_{21}^2\xi^2 \\ 0 & 1 & 0 & \vdots & 0 & \xi & 0 & 0 & \eta & 0 & 0 & \xi\eta & 0 & \vdots & j_{12}^2\eta^2 & j_{22}^2\xi^2 \\ 0 & 0 & 1 & \vdots & 0 & 0 & \xi & 0 & 0 & \eta & 0 & 0 & \xi\eta & \vdots & j_{11}j_{12}\eta^2 & j_{21}j_{22}\xi^2 \end{bmatrix} \begin{Bmatrix} \beta_1 \\ \vdots \\ \beta_{14} \end{Bmatrix} \quad (23)$$

The quadratic membrane element has 16 degrees of freedom. Therefore, a stress field with a minimum of 13 independent parameters is needed to describe the membrane stress field. In results, the above stress assumption, without changing the stress values, can be expressed in a matrix form as

$$\boldsymbol{\sigma}_e = \mathbf{P} \cdot \boldsymbol{\beta} = (\mathbf{I}_c + \mathbf{P}_{h1} + \mathbf{T}_0 \mathbf{P}_{h2}^*) \boldsymbol{\beta} \quad (24)$$

where

$$\mathbf{T}_0 = \begin{bmatrix} j_{11}^2 & j_{21}^2 & 2j_{11}j_{21} \\ j_{12}^2 & j_{22}^2 & 2j_{12}j_{22} \\ j_{11}j_{12} & j_{21}j_{22} & j_{11}j_{22} + j_{12}j_{21} \end{bmatrix}, \quad \mathbf{P}_{h2}^* = \begin{bmatrix} \eta^2 & 0 \\ 0 & \xi^2 \\ 0 & 0 \end{bmatrix}$$

The matrix \mathbf{T}_0 is a transformation matrix, evaluated at the origin, $(\xi, \eta) = (0, 0)$, in the natural coordinate system, which transforms the covariant stresses defined in the natural coordinate to the physical stress defined in the Cartesian coordinate. This approach of obtaining optimal stress terms by using the non-compatible modes of Eq. (19) and the constraint Eq. (12) is equivalent to that of defining the covariant stresses only with the assumption matrix \mathbf{P} and then transforming them to the physical components by transformation matrix calculated at the point (Yeo and Lee 1997).

5. General formulation of hybrid stress elements

The variational basis of hybrid stress formulation is the Hellinger-Reissner principle with constraint equations for assumed stresses. Following Pian and Wu (1988), when the terms corresponding to applied loads are neglected, the Hellinger-Reissner functional can be expressed as

$$\Pi_{HR} = -\frac{1}{2} \int_{\Omega} \boldsymbol{\sigma}^T \mathbf{S} \boldsymbol{\sigma} d\Omega + \int_{\Omega} \boldsymbol{\sigma}^T (D\mathbf{u}) d\Omega \quad (25)$$

where Ω is the domain of the element; \mathbf{S} is the material compliance matrix, D is the strain-displacement operator, \mathbf{u} is the total displacements, $\mathbf{u} = \mathbf{u}_q + \mathbf{u}_\lambda$, with \mathbf{u}_q as the compatible displacements in terms of nodal displacements and \mathbf{u}_λ the non-conforming(incompatible) displacements in terms of internal displacements. $\boldsymbol{\sigma}$ is the vector of assumed stresses.

For finite element approximation, displacements and assumed stresses for one element are discretized as follows

$$\mathbf{u} = \mathbf{N} \mathbf{d} \quad (26)$$

$$\boldsymbol{\sigma} = \mathbf{P} \boldsymbol{\beta} \quad (27)$$

where $\boldsymbol{\beta}$ is the vector of assumed stress parameters. \mathbf{N} is the matrix of standard isoparametric shape functions defined in the natural coordinate system, and \mathbf{P} is the matrix of basis functions for stress assumption.

Substituting Eqs. (26) and (27) into Eq. (25), we can get the following matrix form of the discretized Hellinger-Reissner functional

$$\Pi_{HR} = -\frac{1}{2}\beta^T \mathbf{H}\beta + \beta^T \mathbf{G}\mathbf{d} \quad (28)$$

in which

$$\begin{aligned} \mathbf{H} &= \int_{\Omega} \mathbf{P}^T \mathbf{S} \mathbf{P} d\Omega \\ \mathbf{G} &= \int_{\Omega} \mathbf{P}^T \mathbf{B} d\Omega \quad (\mathbf{B} = \mathbf{D} \cdot \mathbf{N}) \end{aligned}$$

The element stiffness equation will be given by the system stationary condition. The element level relation between stress parameters and nodal displacements is given as:

$$\beta = -\mathbf{H}^{-1} \mathbf{G} \cdot \mathbf{d} \quad (29)$$

$$\mathbf{K} = \mathbf{G}^T \mathbf{H}^{-1} \mathbf{G}, \quad \mathbf{K} \cdot \mathbf{d} = \mathbf{f} \quad (30)$$

A 3×3 Gauss-Legendre full integration is used for the evaluation of the element stiffness matrix.

6. Numerical results

The performance of the hybrid stress element is evaluated in this section. Some of the numerical examples included here are often used as benchmarks for the numerical behavior of the quadrilateral elements. In all the examples, the material is assumed to be linear, elastic, homogeneous, and isotropic. All units of model data are assumed to be consistent, and therefore need not be specified.

Table 1 List of finite elements used for comparison

Name	Description
Q4	Standard 4-node bilinear isoparametric plane element.
Q8	Standard 8-node quadratic plane element.
QPM8	2D plane stress continuum element in LUSAS
QC9D	Membrane finite element with drilling degrees of freedom derived by Groenwold and Stander (1995).
5β-EP	5β family with equilibrium constraint plus perturbation derived by Di and Ramm (1994).
5β-NT	5β family with normalized transformed derived by Di and Ramm (1994).
8β-EP	8β family with equilibrium constraint plus perturbation derived by Geyer and Groenwold (2002).
M5β	4-node plane element with refined transformation matrix derived by Yeo and Lee (1997).
XSHELL42	4-node assumed strain quasi-conforming shell element with 6 degrees of freedom derived by Kim <i>et al.</i> (2003)
8-SAP	8-node serendipity element with explicit and assumed strains formulation, modified shape functions, and refined first-order theory derived by Chun and Kassegne (2005)
HQ8-14β	Present hybrid assumed stress 8-node plane element with non-conforming displacement modes and modified shape functions

Table 2 Eigenvalue

λ_i	Eigenvalue
1	4.5939E-00
2	4.5939E-00
3	2.1333E-00
4	2.1031E-00
\vdots	\vdots
12	3.0155E-01
13	1.5621E-01
14	1.0000E-07
15	-5.0000E-08
16	-5.0000E-08

It is shown that the results from the proposed element developed here show very good agreement with those reported in the literature. A list of plane elements used for comparison with the proposed element is outlined in Table 1.

6.1 Eigenvalue test

The eigenvalue analyses of the elements have been performed in order to check the presence of spurious zero energy modes. The plane stress elements must have 3-rigid body mode on an element without constraints. Therefore three of the λ_i should be zero for a plane element.

The single meshed model has a thickness of 1.0 and side lengths of 1.0. The material properties are $E = 1.0$ and $\nu = 1.0$. The results of the patch test are presented in Table 2. The new proposed element, HQ8-14 β , is pass the patch tests performed.

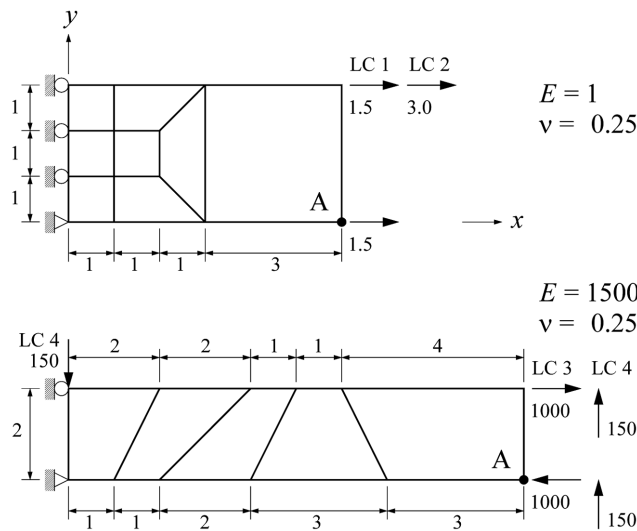


Fig. 3 Patch test and cantilever beam

Table 3 Patch test and cantilever beam

Element	LC1	LC2	LC3			LC4	
	u_{1_A}	$-u_{2_A}$	u_{2_A}	$-\sigma_{x_B}$	$-\tau_{xy_B}$	u_{2_A}	$-\sigma_{x_B}$
Q8	6.00	17.80	99.70	3003	2.72	101.41	4095
QC9D	6.00	16.78	81.86	2541	-	84.59	3433
5β -EP	6.00	17.64	96.18	3014	-	98.19	4137
8β -EP	6.00	16.87	84.86	2881	-	88.00	3822
8-SAP	6.00	17.79	99.75	-	-	101.79	-
HQ8- 14β	6.00	17.75	100.00	3000	0.00	102.13	4137
Analytical	6.00	18.00	100.00	3000	0.00	102.00	4050

6.2 Patch test and cantilever beam

The effect of mesh distortion on finite element accuracy is studied by using the two-element cantilever beam. The geometry is depicted in Fig. 3, and the numerical results are presented in Table 3. Load case 1 represents a patch test, which is passed by all the elements studied. Load case 2 represents bending behavior, while load cases 3 and 4 examine the effect of element distortion.

The new proposed element, HQ8- 14β , is more accurate than not only the quadratic elements Q8 but also the membrane elements with drilling rotational degree of freedom, QC9D. The Q8 and 8-SAP elements yields slightly better results for a load case 2 only.

6.3 Tapered and swept beam

A tapered, swept beam with one edge clamped and the opposite edge acted upon by a unit load at the tip is shown in Fig. 4. The elements used to model the beam are distorted and are under membrane forces. The beam is analyzed by using 2×2 , 4×4 , and 8×8 meshes. The normalized vertical deflection δ_c at point C are presented in Table 4. The reference solution, 23.91, is obtained by Simo *et al.* (1989). The normalized Max. and Min. principal stresses at point A and B are presented in Table 5. Tables shows that the present element, HQ8- 14β , is the most accurate elements.

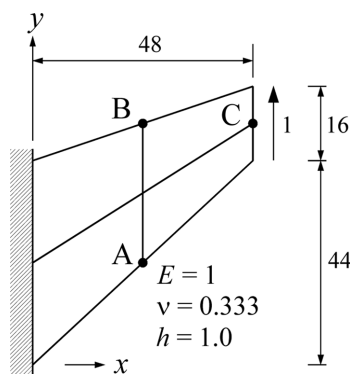


Fig. 4 Tapered and swept beam

Table 4 Normalized results for the tapered and swept beam

Element	2×2	4×4	8×8
Q4	0.496	0.765	0.923
Q8	0.950	0.992	0.999
QC9D	0.806	0.946	0.985
5 β -EP	0.884	0.963	0.991
8 β -EP	0.841	0.950	0.986
8-SAP	0.953	0.992	0.999
HQ8-14 β	0.968	0.993	0.999

Table 5 Maximum and minimum principal stresses

Element	2×2 mesh		4×4 mesh		8×8 mesh	
	$(\sigma_{\max})_A$	$(\sigma_{\min})_B$	$(\sigma_{\max})_A$	$(\sigma_{\min})_B$	$(\sigma_{\max})_A$	$(\sigma_{\min})_B$
Q8	1.057	1.044	1.025	1.002	1.012	1.013
QC9D	0.779	0.804	0.950	0.948	0.984	1.001
5 β -EP	0.786	0.778	0.950	0.924	0.994	0.988
8 β -EP	0.768	0.818	0.959	0.906	0.998	0.990
HQ8-14 β	1.099	1.065	1.031	1.004	1.012	1.013
Analytical	0.2360	-0.2010	0.2360	-0.2010	0.2360	-0.2010

6.4 Element distortion sensitivity test

A cantilever beam of two elements with different distortions is a well-known example for testing the sensitivity of the element to mesh distortion. Here, the effect of mesh distortion on the HQ8-14 β element accuracy is investigated by using the two-element cantilever beam shown in Figs. 5 and 8. The normalized vertical deflections at tip point A and B is plotted in Figs. 6 and 9 versus the parameter e , which represents the degree of geometric distortion of the two elements. Although all elements except for the Q4, yield the exact solution when there is no geometric distortion, $e = 0$, it is seen that their performance under severe distortion is quite different. The results show that for the vertical displacement at point A and B, the present element, HQ8-14 β , give very exact solutions even when the elements are highly distorted.

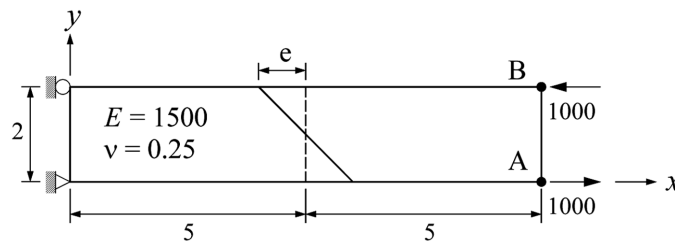


Fig. 5 Element distortion test under end moment

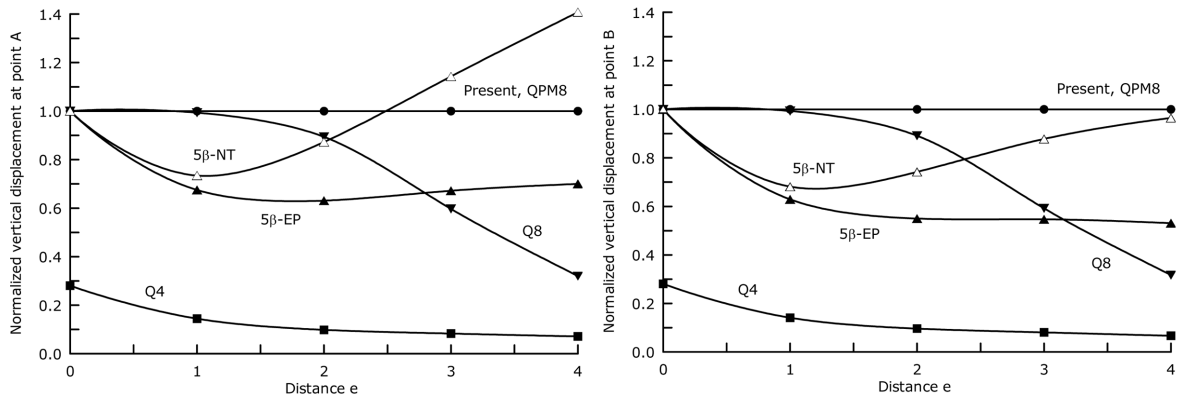


Fig. 6 Normalized results of element distortion test under end moment

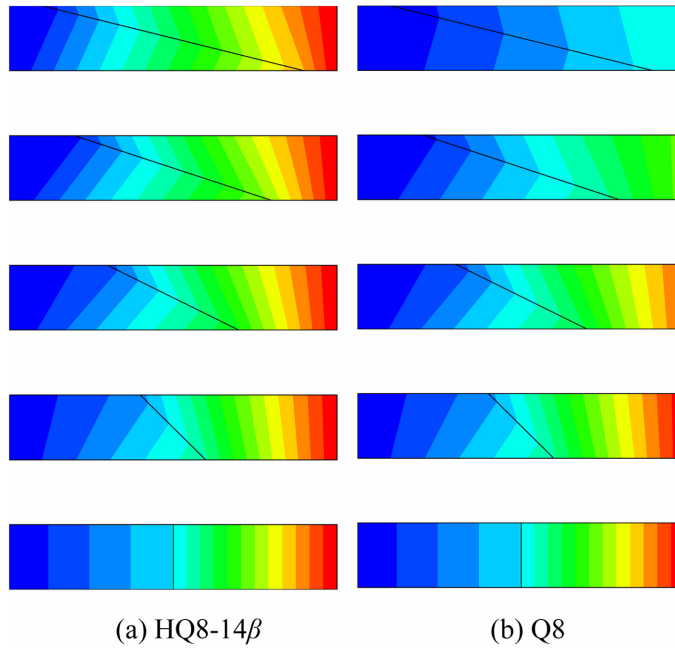


Fig. 7 Vertical displacement contour for element distortion

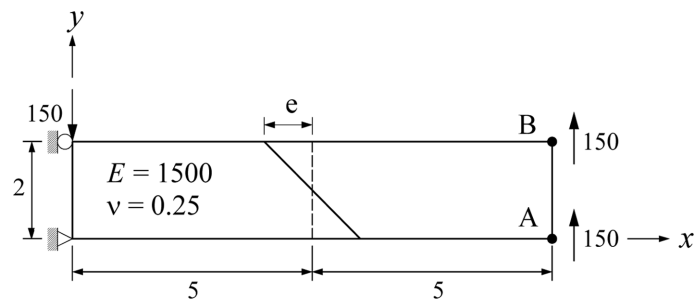


Fig. 8 Element distortion test under end shear

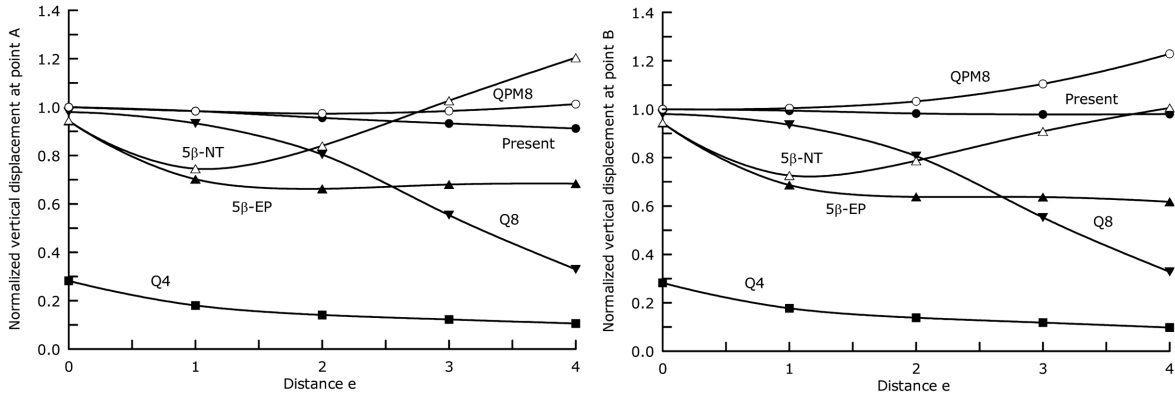


Fig. 9 Normalized results of element distortion test under end shear

6.5 Straight cantilever beams

The straight cantilever beam problem suggested by MacNeal and Harder (1985) is solved for the three discretizations shown in Fig. 10. The theoretical results for extension and in-plane shear are simply calculated from the elementary beam theory including shear deformations. The problem is solved to demonstrate the elements capability in handling meshes with distortions and high aspect ratios. For extension problem, the results show that all elements perform well. For in-plane shear problem, the result of HQ8-14β shows less sensitivity to mesh distortion compared with M5β, Q8 and 8-SAP. However, for the regular shaped elements, M5β provides better results. The present element has the error of fewer than 3.0% for all meshes and loads.

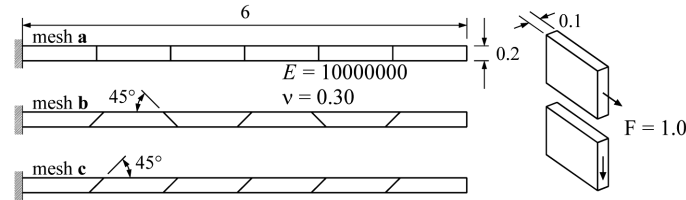


Fig. 10 Straight cantilever beam

Table 6 Normalized results to the straight beam

Tip load direction	Element	Theoretical solution	mesh a	mesh b	mesh c
Extension	M5β	3.0×10^{-5}	1.000	1.000	1.000
	Q8		0.998	0.998	0.998
	8-SAP		0.998	0.998	0.998
	HQ8-14β		1.000	1.000	1.000
In-plane shear	M5β	0.1081	1.000	0.378	0.957
	Q8		0.982	0.899	0.980
	8-SAP		0.962	0.971	0.982
	HQ8-14β		0.987	0.975	0.987

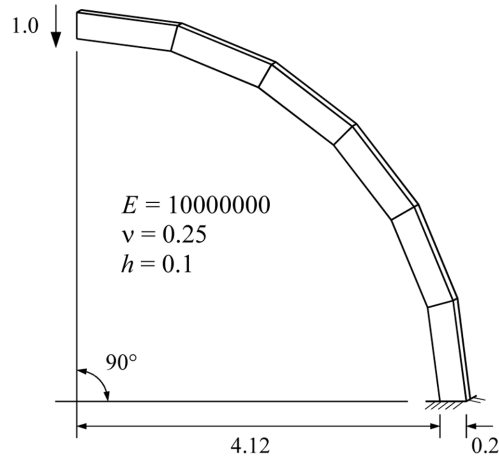


Fig. 11 Curved cantilever beam

Table 7 Normalized results to the curved cantilever beam

Element	In-plane shear
5β -NT	0.07751 (0.887)
XSHELL42	0.08341 (0.955)
HQ8- 14β	0.08786 (1.006)
Theoretical solution	0.08734

6.6 Curved cantilever beam subjected to end in-plane shear

The curved cantilever beam is formed by a 90° circular arc. An in-plane load is applied at the free end of beam. A coarse mesh of 1×6 that results in a high aspect ratio for each element is adopted. The normalized results from the present element, HQ8-14β, and other elements are tabulated in Table 7. In this problem, it is clear that the results for all elements except the 5β-NT are uniformly good. However, the HQ8-14β consistently performs better than the other elements, as shown in the table.

7. Conclusions

In this paper, we have presented a new hybrid element model through the use of non-conforming displacement modes and modified shape functions. The new element consists of two additional non-conforming modes that are added to the translational degree of freedom to improve the behavior of a membrane component. Further, the modification of the shape functions through quadratic polynomials in x - y coordinates enables retaining reasonable accuracy even when the element becomes considerably distorted. The new and refined 8-node hybrid stress plane element presented here is compared with existing elements to establish its accuracy and efficiency. Over a wide range of mesh distortions, the element presented here is found to be exceptionally accurate in predicting displacements.

References

- Chun, K.S. and Kassegne, S.K. (2005), "A new efficient 8-node Serendipity element with explicit and assumed strain formulations", *Int. J. Comput. Eng. Sci.*, **6**(4), 285-292.
- Choi, C.K., Lee, P.S. and Park, Y.M. (1999), "Defect-free 4-node flat shell element: NMS-4F element", *Struct. Eng. Mech.*, **8**(2), 207-231.
- Choi, C.K. and Park, Y.M. (1999), "Quadratic NMS Mindlin-plate-bending element", *Int. J. Numer. Meth. Eng.*, **46**, 1273-1289.
- Chen, W. and Cheung, Y.K. (1995), "A robust refined quadrilateral plane element", *Int. J. Numer. Meth. Eng.*, **38**, 649-666.
- Di, S. and Ramm, E. (1994), "On alternative hybrid stress 2D and 3D elements", *Eng. Comput.*, **11**, 49-68.
- Feng, W., Hoa, S.V. and Huang, Q. (1997), "Classification of stress modes in assumed stress fields of hybrid finite elements", *Int. J. Numer. Meth. Eng.*, **40**, 4313-4339.
- Groenwold, A.A. and Stander, N. (1995), "An efficient 4-node 24 D.O.F. thick shell finite element with 5-point quadrature", *Eng. Comput.*, **12**, 723-747.
- Geyer, S. and Groenwold, A.A. (2002), "Two hybrid stress membrane finite element families with drilling rotations", *Int. J. Numer. Meth. Eng.*, **53**, 583-601.
- Kim, K.D., Lomboy, G.R. and Voyiadjis, G.Z. (2003), "A 4-node assumed strain quasi-conforming shell element with 6 degrees of freedom", *Int. J. Numer. Meth. Eng.*, **58**, 2177-2200.
- Kikuchi, F., Okabe, M. and Fujio, H. (1999), "Modification of the 8-node serendipity element", *Comput. Meth. Appl. Mech. Eng.*, **179**, 91-109.
- MacNeal, R.H. and Harder, R.L. (1985), "A proposed standard set of problems to test finite element accuracy", *Finite Elem. Anal. D.*, **1**, 3-20.
- MacNeal, R.H. and Harder, R.L. (1992), "Eight nodes or nine?", *Int. J. Numer. Meth. Eng.*, **33**, 1049-1058.
- Pian, T.H.H. (1964), "Derivation of element stiffness matrices by assumed stress distributions", *AIAA J.*, **2**, 1333-1376.
- Pian, T.H.H. and Sumihara, K. (1984), "Rational approach for assumed stress finite elements", *Int. J. Numer. Meth. Eng.*, **20**, 1685-1695.
- Pian, T.H.H. and Tong, P. (1986), "Relation between incompatible displacement model and hybrid stress model", *Int. J. Numer. Meth. Eng.*, **22**, 173-181.
- Pian, T.H.H. and Wu, C.C. (1988), "A rational approach for choosing stress terms for hybrid finite element formulations", *Int. J. Numer. Meth. Eng.*, **26**, 2331-2343.
- Simo, J.C., Fox, D.D. and Rifai, M.S. (1989), "On stress resultant geometrically exact shell model. Part II: The linear theory; computational aspects", *Comput. Meth. Appl. Mech. Eng.*, **73**, 53-92.
- Sze, K.Y. (1992), "Efficient formulation of robust mixed element using orthogonal stress/strain interpolants and admissible matrix formulation", *Int. J. Numer. Meth. Eng.*, **35**, 1-20.
- Taylor, R.L., Beresford, P.J. and Wilson, E.L. (1976), "A nonconforming element for stress analysis", *Int. J. Numer. Meth. Eng.*, **10**, 1211-1219.
- Wu, C.C. and Cheung, Y.K. (1995), "On optimization approaches of hybrid stress elements", *Finite Elem. Anal. D.*, **21**, 111-128.
- Wu, C.C. and Cheung, Y.K. (1996), "Penalty-equilibrating approach and an innovation of 4-noded hybrid stress elements", *Commun. Numer. Meth. Eng.*, **12**, 707-717.
- Wilson, E.L., Taylor, R.L., Doherty, W.P. and Ghaboussi, J. (1973), "Incompatible displacement models", *Numer. Comput. Meth. Struct. Mech.* (Ed Fenves *et al.*), Academic Press. New York.
- Yeo, S. and Lee, B.C. (1997), "New stress assumption for hybrid stress elements and refined four-node plane and eight-node brick elements", *Int. J. Numer. Meth. Eng.*, **40**, 2933-2952.